LETTERS
PUBLISHED ONLINE: 18 APRIL 2016 | DOI: 10.1038/NPHYS3722
nature physics

Atomic spin-chain realization of a model for quantum criticality

R. Toskovic[1†], R. van den Berg[2†], A. Spinelli[1], I. S. Eliens[2], B. van den Toorn[1], B. Bryant[1], J.-S. Caux[2] and A. F. Otte[1*]

The ability to manipulate single atoms has opened up the door to constructing interesting and useful quantum structures from the ground up[1]. On the one hand, nanoscale arrangements of magnetic atoms are at the heart of future quantum computing and spintronic devices[2,3]; on the other hand, they can be used as fundamental building blocks for the realization of textbook many-body quantum models[4], illustrating key concepts such as quantum phase transitions, topological order or frustration as a function of system size. Here, we use low-temperature scanning tunnelling microscopy to construct arrays of magnetic atoms on a surface, designed to behave like spin-1/2 XXZ Heisenberg chains in a transverse field, for which a quantum phase transition from an antiferromagnetic to a paramagnetic phase is predicted in the thermodynamic limit[5]. Site-resolved measurements on these finite-size realizations reveal a number of sudden ground state changes when the field approaches the critical value, each corresponding to a new domain wall entering the chains. We observe that these state crossings become closer for longer chains, suggesting the onset of critical behaviour. Our results present opportunities for further studies on quantum behaviour of many-body systems, as a function of their size and structural complexity.

Since the birth of quantum mechanics, lattice spin systems[6] have represented a natural starting point for understanding collective quantum dynamics. Today, scanning tunnelling microscopy (STM) techniques allow one to experimentally build and probe realizations of exchange-coupled lattice spins in different geometries[7–9]. In linear arrangements, quantum effects are strongest[10] and notions such as quantum phase transitions[11] are most easily understood, the simplest illustration being the Ising model in a transverse field[12,13]. In this work, using STM, we construct finite-size versions of a model in the same universality class, namely the spin-1/2 XXZ chain in a transverse field[5], which has previously been realized in the bulk material Cs_2CoCl_4 (refs 14,15). Our set-up allows us to probe the chains with single-spin resolution while tuning an externally applied transverse field through the critical regime.

The chains are created by manipulating Co atoms evaporated onto a Cu_2N/Cu(100) surface (see Methods), which provides efficient decoupling for the magnetic d-shell electrons from the underlying bulk electrons[7]. Employing inelastic electron tunnelling spectroscopy (IETS)[16,17] at sufficiently low temperature (330 mK) allows us to determine the magnetic anisotropy vector of each atom[18] as well as the strength of the exchange coupling between neighbouring atoms[19]. It was previously demonstrated that Co atoms on this surface behave as spin $S=3/2$ objects experiencing a strong uniaxial hard-axis anisotropy pointing in-plane, perpendicular to the bond with the neighbouring N atoms[20]. As a result, the $m_z=\pm 3/2$ states split off approximately 5.5 meV above the $m_z=\pm 1/2$ doublet (see Fig. 1a). As we will show below, by exploiting the magneto-crystalline anisotropy, we thus effectively reduce the spins from 3/2 to 1/2. The Cu_2N islands were kept small (∼6 nm) to ensure limited variation in anisotropy and substrate coupling between different atoms inside the chains[21].

The Co atoms are manipulated into the arrangement shown in Fig. 1b, such that their interaction is governed by the spin-3/2 nearest neighbour antiferromagnetic isotropic Heisenberg exchange:

$$\mathcal{H}_{3/2}=J\sum_{i=1}^{N-1}\mathbf{S}_i\cdot\mathbf{S}_{i+1}+D\sum_{i=1}^{N}(S_i^z)^2-g\mu_B B_x\sum_{i=1}^{N}S_i^x \qquad (1)$$

with interaction strength $J=0.24$ meV (ref. 22), subjected to an external magnetic field $\mathbf{B}$ (with g-factor $g=2.3$ (ref. 20)) applied perpendicular to the surface. This weak interaction was chosen specifically from a set of possible configurations[22] to provide a critical point at an accessible field value. Because J and all other relevant energy scales (k_BT, μ_BB) stay well below the anisotropy energy $2D\approx 5.5$ meV, excitations to $\pm 3/2$ doublets can be projected out through a Schrieffer–Wolff transformation up to first order in $1/D$ (refs 15,23,24). This results in an effective spin-1/2 Hamiltonian:

$$\mathcal{H}_{1/2}=\sum_{i=1}^{N-1}J_\perp(S_i^xS_{i+1}^x+S_i^yS_{i+1}^y)+J_zS_i^zS_{i+1}^z$$
$$+J_\perp^{\mathrm{nnn}}\sum_{i=1}^{N-2}S_i^xS_{i+2}^x+S_i^yS_{i+2}^y-\mu_BB_x\sum_{i=1}^{N}g_iS_i^x \qquad (2)$$

with nearest and next-nearest neighbour exchange parameters and bulk/boundary g-factors given by:

$$J_\perp=4J,\quad J_z=J-\frac{39J^2}{8D},\quad J_\perp^{\mathrm{nnn}}=-\frac{3J^2}{D},$$

$$g_i=\begin{cases}2g\left(1-\dfrac{3J}{2D}\right) & \text{if } i=2,\ldots,N-1\\ 2g\left(1-\dfrac{3J}{4D}\right) & \text{if } i=1,N\end{cases} \qquad (3)$$

[1]Department of Quantum Nanoscience, Kavli Institute of Nanoscience, Delft University of Technology, Lorentzweg 1, 2628 CJ Delft, The Netherlands. [2]Institute for Theoretical Physics, University of Amsterdam, Science Park 904, 1090 GL Amsterdam, The Netherlands. †These authors contributed equally to this work. *e-mail: a.f.otte@tudelft.nl

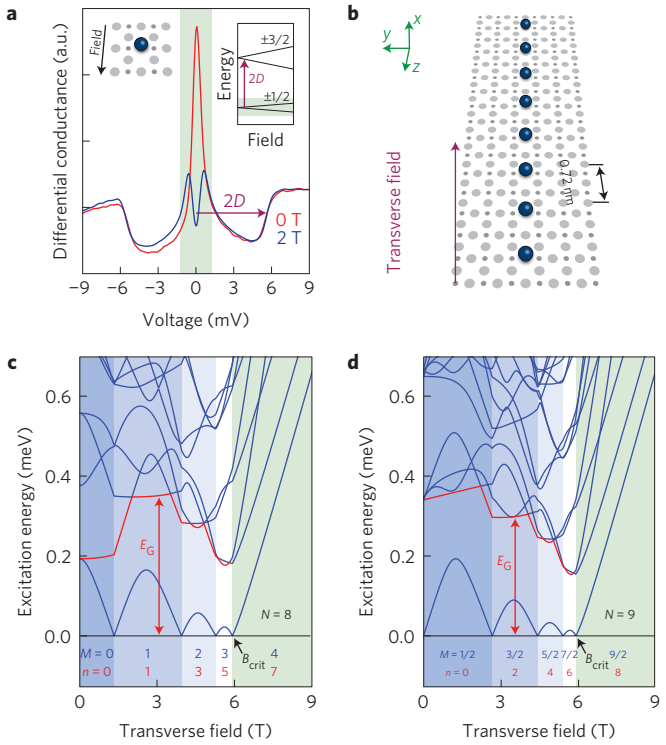

Figure 1 | Construction of XXZ chains. a, IETS spectra taken on a single Co atom on Cu_2N at 0 T and 2 T applied along the hard axis. Left inset: atomic arrangement near the Co atom. Right inset: energy diagram indicating the separation between the ±1/2 and ±3/2 doublets. **b**, Atomic design for XXZ chains and indication of the transverse field direction. Large (small) grey circles represent Cu (N) atoms. **c**, Lowest excitation energies of an $N=8$ chain for a transverse field up to 9 T. E_G and B_{crit} are indicated, as well as the transverse magnetization M and average number of domain walls n between each ground state change. **d**, Same as **c** for $N=9$.

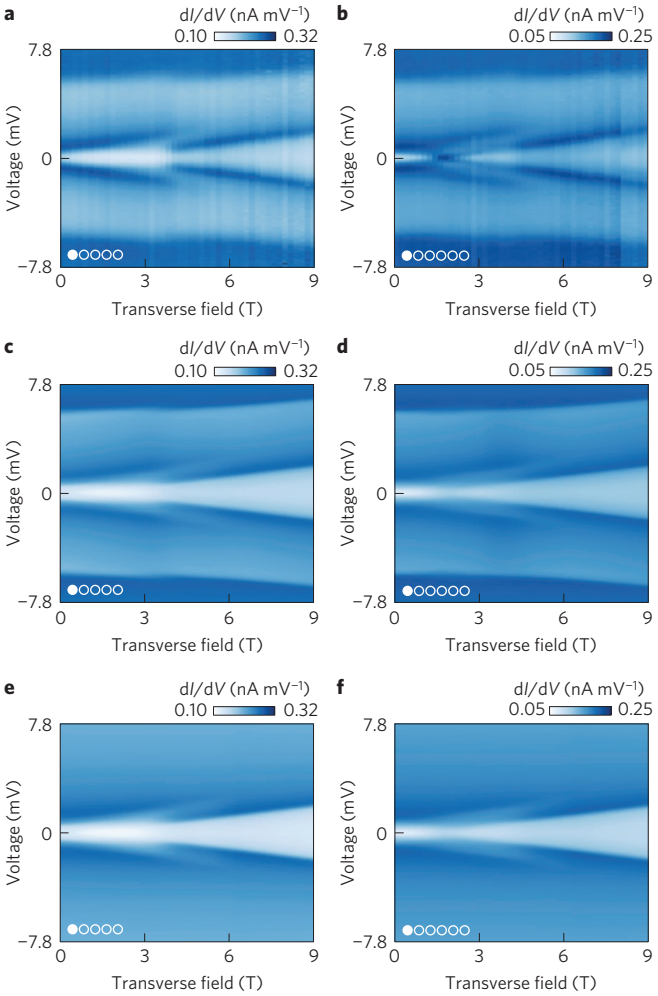

Figure 2 | Comparison to theory. a, IETS spectra taken on atom 1 of an $N=5$ chain in transverse fields ranging from 0 T to 9 T, in increments of 200 mT. **b**, Same as **a**, but taken on atom 1 of an $N=6$ chain. IETS curves were normalized to correct for tip height variations. Conductance values listed at the colour bars are indicative only: owing to normalization, scaling between spectra may vary by ~20%. **c**,**d**, Theoretical spectra corresponding to **a**,**b**, respectively, calculated using a spin-3/2 model (equation (1)). The Kondo peak appearing at the first ground state crossing in **b** is under-represented in the theory (**d**). **e**,**f**, Same as **c**,**d**, but calculated using a spin-1/2 XXZ model (equation (2)).

The model $H_{1/2}$ with $J_{\perp}^{nnn}=0$, uniform g_i and $J_z/J_{\perp}\approx 1/8$ has a phase transition at $g_i\mu_B B_x \approx 1.5J_{\perp}$ from an antiferromagnetic to a paramagnetic phase[5]. The additional next-nearest neighbour coupling $J_{\perp}^{nnn}$ generated by the Schrieffer–Wolff transformation affects neither the qualitative features of the spectrum nor the existence of the phase transition, effectively reducing $H_{1/2}$ to an XXZ Hamiltonian in a transverse field. For finite-size realizations the antiferromagnetic phase is characterized by a number of level crossings, where the ground state switches between sectors of even and odd total magnetization, reflecting the Z_2 symmetry corresponding to a π-rotation of all spins around the field axis[25].

Figure 1c,d shows the calculated lowest excitation energies of $H_{1/2}$ for an even-numbered ($N=8$) and an odd-numbered ($N=9$) chain, respectively, for a transverse field up to 9 T. Below the transition to the paramagnetic phase, just below 6 T, several ground state crossings are predicted, with their number increasing with chain length. Starting from a state with Néel-like order near zero field, each crossing corresponds to a stepwise increase of the total magnetization M along the field and the average number of antiferromagnetic domain walls n inside the chain (Supplementary Fig. 1).

The lowest excited state is energetically distinguishable in finite chains, but becomes degenerate with the ground state in the thermodynamic limit, where it corresponds (through a Jordan–Wigner transformation[26,27]) to the topological edge states recently observed in ferromagnetic chains on a superconducting surface[28]. Below the critical field B_{crit}, the ground state and this zero mode are separated from the higher excited states by an energy gap E_G. As the length of the chain increases, E_G remains finite and forms the characteristic energy separating the ground state from the continuum—except at B_{crit}, where it vanishes. Just below this point, spin liquid behaviour is predicted[5].

We constructed chains of Co atoms of various length and performed low-temperature IETS measurements ($T=330\,mK<E_G/k_B$) on each atom in a chain while varying the strength of the transverse field. To obtain an extensive data set, a fully automated measurement sequence was employed (see Methods). Figure 2a,b shows measurements taken on the first atom of an odd-length (5 atoms) and an even-length chain (6 atoms), respectively, recorded for every 200 mT from 0 to 9 T. At voltages below 5.5 mV, transitions within the manifold of $m_z=\pm 1/2$ states are observed; excitations at higher voltages correspond to transitions to the $m_z=\pm 3/2$ manifold. The spectra show sudden changes in both excitation energy and intensity at field values corresponding to expected ground state crossings: near 3.5 T for $N=5$ and near 1.5 T and 4.0 T for $N=6$.

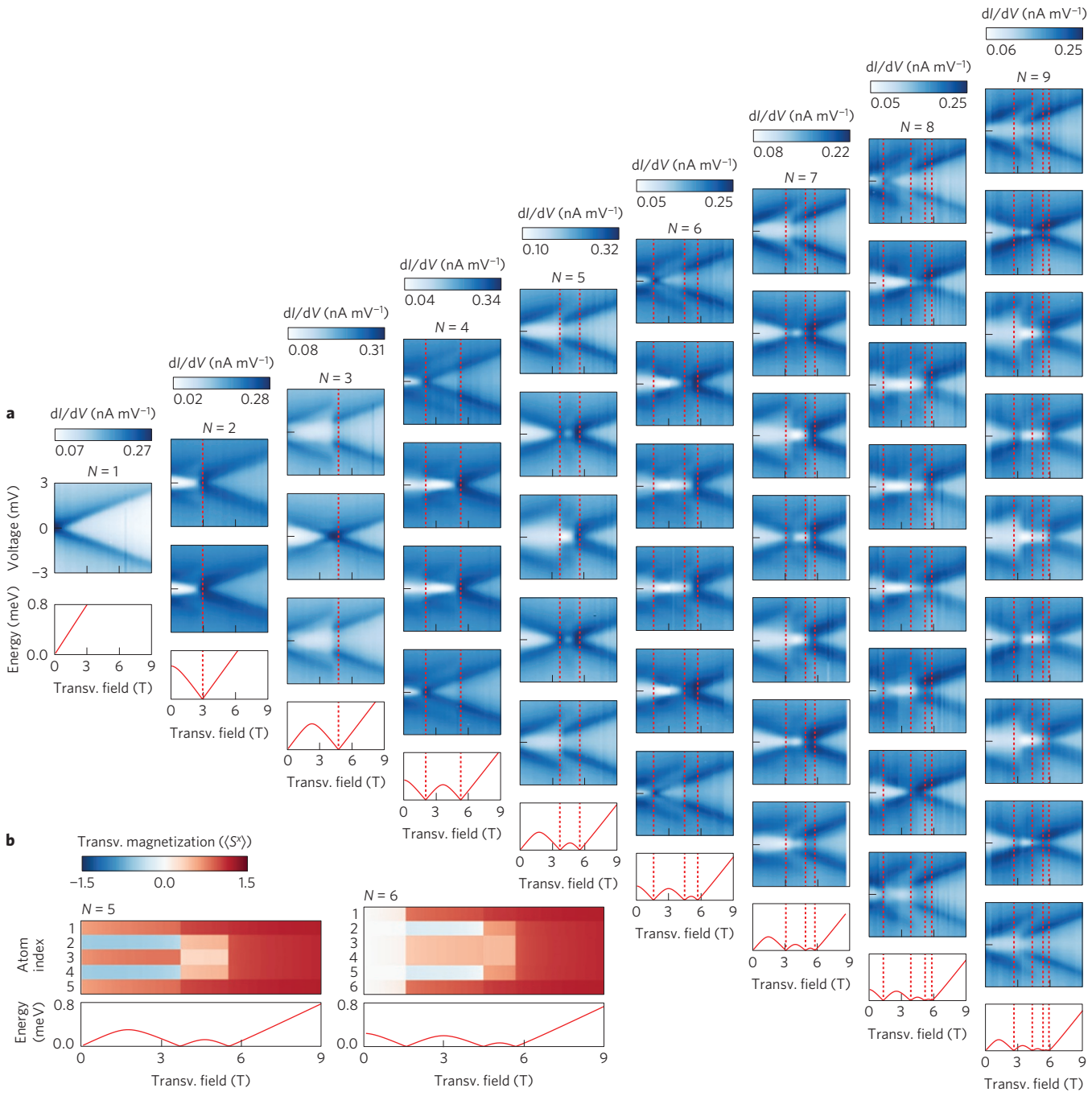

Figure 3 | Experimental results on chains of one to nine atoms. a, IETS spectra from 0 T to 9 T transverse field (in 200 mT increments) obtained on each atom of every chain up to a length of nine atoms (up to 8.6 T for $N=7$). Calculated lowest excitation energies are shown below each chain data set. Red dashed lines indicate positions of expected calculated ground state crossings. Owing to normalization, scaling of individual spectra may differ by ~20% from values listed at the colour bars. **b**, Site-resolved transverse magnetization ($\langle S^x \rangle$) for $N=5$ and $N=6$ as calculated from the $H_{3/2}$ model. Excitation energies (red) same as in **a**.

To simulate the shape of the differential conductance spectra, we employed a perturbative transport model[17,22,29,30]. Steps related to the spectrum are found in good agreement with the data using the $S=3/2$ Hamiltonian (equation (1); Fig. 2c,d). Calculations using the $S=1/2$ XXZ Hamiltonian (equation (2); Fig. 2e,f) show similar agreement, except for the excitations to the $m_z=\pm 3/2$ multiplet near ± 5.5 mV, which are not modelled. This agreement justifies our effective spin-1/2 treatment. A notable quantitative discrepancy between theory and experiment is found near 1.5 T in the $N=6$ chain. At this field value, a two-fold ground state degeneracy occurs, resulting in a zero-bias Kondo resonance in the data, which is only partly reproduced in the third-order perturbative analysis[22,30–33].

In Fig. 3a, field-dependent measurements are shown for all atoms of chains of 1 to 9 atoms, featuring a total of 2,056 IETS spectra. Here, we focus on the ± 3 mV range corresponding to the $m_z=\pm 1/2$ multiplets. As chain length increases, more features become visible, each marking a change of the ground state as the field is increased. When comparing these to the calculated ground state crossing positions (lower panels), we find that for chains up to length $N=6$ each feature lines up with one of the crossings. The IETS data also

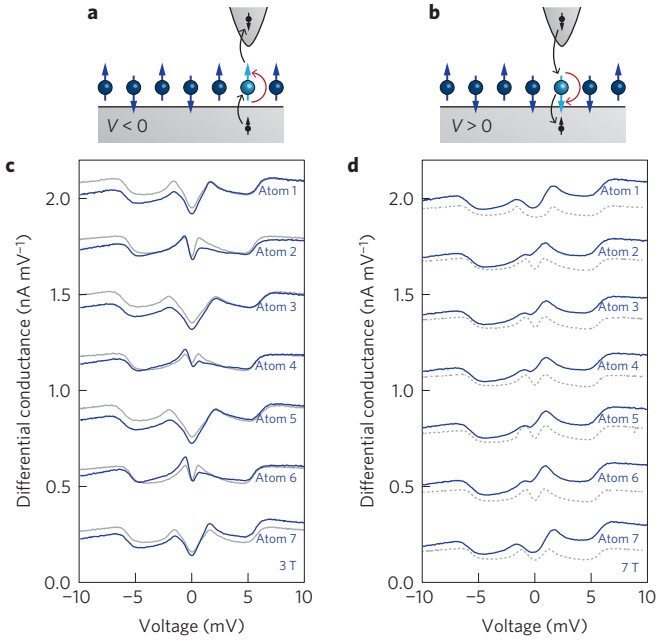

Figure 4 | Spin-polarized spectroscopy. a,**b**, Schematics showing allowed spin excitations in the case of a fully polarized (in the spin-down direction, see Supplementary Fig. 4) STM tip for negative and positive sample voltages, respectively. **c**, Spin-polarized IETS spectra taken in a 3 T transverse field on an $N=7$ chain (blue curves). Corresponding spectra taken with an unpolarized tip are shown in grey. **d**, Same as **c**, but in a 7 T transverse field. Here the unpolarized data (dotted grey lines) were taken on a different, but identical chain.

reveal the positions within each chain which are affected most by each of the ground state crossings; these findings are supported by local magnetization calculations along the field direction (Fig. 3b and Supplementary Fig. 2).

For longer chains, the positions of the gap closings in the IETS data deviate slightly from the calculated values, although qualitatively the observed data evolve as expected. A possible explanation for this discrepancy is the presence of long-range interactions: including an additional ferromagnetic next-nearest neighbour coupling of $0.05J$ gives a better agreement with the data even in longer chains (see Supplementary Fig. 3). However, we believe that a number of other effects may contribute to the discrepancy as well; a full resolution of the mismatch would necessitate an extensive study of both the electronic and magnetic properties of the substrate and the adatoms.

On atoms in the bulk of the chain (two or more sites away from an edge), a continuous featureless region is observed between 3 T and 6 T, which widens as chain length increases. In this field range, ground state crossings become too close to be individually resolved. The energy difference between the ground state and the zero mode also decreases, such that their thermal occupations become comparable. This further reduces the ability to resolve the crossings.

A simplified picture in terms of spin-1/2 product states and spin flip operations[8] provides a qualitative understanding of the IETS spectra. In even chains, for small fields, the two Néel orderings are equally mixed in the ground state. Here the first crossing is predominantly found on the outer atoms, because at this crossing the number of domain walls n increases by 1 only. In odd-length chains, the magnetic field selects one of these Néel states leading to a definite staggered magnetization profile: flipping the spin of an odd (even) atom points it against (along) the magnetic field, leading to a state increasing (decreasing) in energy with increasing field. At fields above the critical field, the ground state is essentially polarized and we can obtain a similar understanding in terms of magnon physics.

The semiclassical reasoning outlined above is further confirmed by measurements taken on a seven-atom chain with a spin-polarized (SP) STM tip, shown in Fig. 4. In contrast to SP-STM measurements taken at a fixed voltage, these spectra reveal spin contrast in energy-dependent phenomena such as spin excitations. At 3 T we see, in addition to the even–odd pattern in the excitation energies, an alternating pattern in spin excitation intensities[8] (Fig. 4c). For positive sample bias, in which case an excess of spin-down electrons from the tip is injected into the chain (Supplementary Fig. 4), excitations on odd-site spins are enhanced. At negative voltage, excitations are enhanced on the even sites. This alternating pattern is found to disappear as the field is swept through the critical value (Fig. 4d). Additional SP-STM data are shown in Supplementary Fig. 5.

In conclusion, we have built chains of effective $S=1/2$ spins realizing the XXZ model in a transverse field, and obtained detailed site-resolved information about the spectrum as a function of chain length and applied field. Increasing the chain length shows a growing number of ground state crossings, a precursor of the Ising quantum phase transition occurring in the thermodynamic limit. The origin of the discrepancy between the theoretical positions of ground state crossings and those observed in longer chains remains an open issue that requires a better understanding of the electronic and magnetic structure of the chains and their supporting surface. Our work demonstrates that STM-built spin lattices offer a viable platform, complementary to, for example, ultracold atoms, for experimentally testing quantum magnetism with local precision.

Methods

Methods and any associated references are available in the online version of the paper.

Received 26 August 2015; accepted 9 March 2016; published online 18 April 2016

References

1. Heinrich, A. Atomic spins on surfaces. *Phys. Today* **68,** 42–47 (March, 2015).
2. Wolf, S. A. *et al*. Spintronics: a spin-based electronics vision for the future. *Science* **294,** 1488–1495 (2001).
3. Khajetoorians, A. A., Wiebe, J., Chilian, B. & Wiesendanger, R. Realizing all-spin-based logic operations atom by atom. *Science* **332,** 1062–1064 (2011).
4. Spinelli, A., Rebergen, M. P. & Otte, A. F. Atomically crafted spin lattices as model systems for quantum magnetism. *J. Phys. Condens. Matter* **27,** 243203 (2015).
5. Dmitriev, D. V., Krivnov, V. Y. & Ovchinnikov, A. A. Gap generation in the XXZ model in a transverse magnetic field. *Phys. Rev. B* **65,** 172409 (2002).
6. Heisenberg, W. Zur Theorie des Ferromagnetismus. *Z. Phys. A* **49,** 619–636 (1928).
7. Hirjibehedin, C. F., Lutz, C. P. & Heinrich, A. J. Spin coupling in engineered atomic structures. *Science* **312,** 1021–1024 (2006).
8. Khajetoorians, A. A. *et al*. Atom-by-atom engineering and magnetometry of tailored nanomagnets. *Nature Phys.* **8,** 497–503 (2012).
9. Spinelli, A., Bryant, B., Delgado, F., Fernández-Rossier, J. & Otte, A. F. Imaging of spin waves in atomically designed nanomagnets. *Nature Mater.* **13,** 782–785 (2014).
10. Giamarchi, T. *Quantum Physics in One Dimension* (Oxford Univ. Press, 2003).
11. Sachdev, S. *Quantum Phase Transitions* (Cambridge Univ. Press, 2011).
12. Lieb, E., Schultz, T. & Mattis, D. Two soluble models of an antiferromagnetic chain. *Ann. Phys.* **16,** 407–466 (1961).
13. Elliott, R. J., Pfeuty, P. & Wood, C. Ising model with a transverse field. *Phys. Rev. Lett.* **25,** 443–446 (1970).
14. Kenzelmann, M. *et al*. Order-to-disorder transition in the XY-like quantum magnet Cs_2CoCl_4 induced by noncommuting applied fields. *Phys. Rev. B* **65,** 144432 (2002).
15. Breunig, O. *et al*. Spin-1/2 XXZ chain system Cs_2CoCl_4 in a transverse magnetic field. *Phys. Rev. Lett.* **111,** 187202 (2013).
16. Heinrich, A. J., Gupta, J. A., Lutz, C. P. & Eigler, D. M. Single-atom spin-flip spectroscopy. *Science* **306,** 466–469 (2004).

17. Fernández-Rossier, J. Theory of single-spin inelastic tunneling spectroscopy. *Phys. Rev. Lett.* **102,** 256802 (2009).
18. Hirjibehedin, C. F. *et al*. Large magnetic anisotropy of a single atomic spin embedded in a surface molecular network. *Science* **317,** 1199–1203 (2007).
19. Otte, A. F. *et al*. Spin excitations of a Kondo-screened atom coupled to a second magnetic atom. *Phys. Rev. Lett.* **103,** 107203 (2009).
20. Otte, A. F. *et al*. The role of magnetic anisotropy in the Kondo effect. *Nature Phys.* **4,** 847–850 (2008).
21. Oberg, J. C. *et al*. Control of single-spin magnetic anisotropy by exchange coupling. *Nature Nanotech.* **9,** 64–68 (2014).
22. Spinelli, A. *et al*. Exploring the phase diagram of the two-impurity Kondo problem. *Nature Commun.* **6,** 10046 (2015).
23. Schrieffer, J. R. & Wolff, P. A. Relation between the Anderson and Kondo Hamiltonians. *Phys. Rev.* **149,** 491–492 (1966).
24. MacDonald, A. H., Girvin, S. M. & Yoshioka, D. t/U expansion for the Hubbard model. *Phys. Rev. B* **37,** 9753–9756 (1988).
25. Dmitriev, D. V., Krivnov, V. Y., Ovchinnikov, A. A. & Langari, A. One-dimensional anisotropic Heisenberg model in the transverse magnetic field. *J. Exp. Theor. Phys.* **95,** 538–549 (2002).
26. Kitaev, A. Unpaired Majorana fermions in quantum wires. *Phys.-Usp.* **44,** 131–136 (2001).
27. Thomale, R., Rachel, S. & Schmitteckert, P. Tunneling spectra simulation of interacting Majorana wires. *Phys. Rev. B* **88,** 161103 (2013).
28. Nadj-Perge, S. *et al*. Observation of Majorana fermions in ferromagnetic atomic chains on a superconductor. *Science* **346,** 602–607 (2014).
29. Fransson, J., Eriksson, O. & Balatsky, A. V. Theory of spin-polarized scanning tunneling microscopy applied to local spins. *Phys. Rev. B* **81,** 115454 (2010).
30. Ternes, M. Spin excitations and correlations in scanning tunneling spectroscopy. *New J. Phys.* **17,** 063016 (2015).
31. Kondo, J. Resistance minimum in dilute magnetic alloys. *Prog. Theor. Phys.* **32,** 37–49 (1964).
32. Appelbaum, J. Exchange model of zero-bias tunneling anomalies. *Phys. Rev.* **154,** 633–643 (1967).
33. Zhang, Y. *et al*. Temperature and magnetic field dependence of a Kondo system in the weak coupling regime. *Nature Commun.* **4,** 2110 (2013).

Acknowledgements

This work was supported by FOM, NWO, the Delta ITP consortium and by the Kavli Foundation. We thank M. Ternes for developing the third-order perturbative transport model.

Author contributions

Experiments were performed by R.T., A.S., B.v.d.T. and B.B.; A.F.O. devised the experiments and supervised the work. Theoretical modelling was performed by R.v.d.B., I.S.E. and J.-S.C. All authors contributed to the interpretation of the results and to the writing of the manuscript.

Additional information

Supplementary information is available in the online version of the paper. Reprints and permissions information is available online at www.nature.com/reprints. Correspondence and requests for materials should be addressed to A.F.O.

Competing financial interests

The authors declare no competing financial interests.

Methods

Experimental set-up and measurements. The measurements reported in this paper have been conducted in a commercial low-temperature STM (UNISOKU USM 1300S) at 330 mK and in ultrahigh vacuum (below 2×10^{-10} mbar). A Cu_2N monolayer was prepared *in situ* on a Cu(100) substrate by sputtering N_2 for 45 s at 1×10^{-5} mbar and 500 eV followed by 1 min of annealing at 400 °C, resulting typically in rectangular Cu_2N islands with their most elongated direction being smaller than 10 nm (ref. 34). Co atoms were evaporated at approximately 1,060 °C onto the pre-cooled Cu_2N surface. A PtIr tip was used, which we prepared by e-beam annealing followed by indention into a bare Cu surface. Chains of Co atoms were assembled by means of vertical atom manipulation.

IETS measurements on Co atoms were realized by recording dI/dV spectra employing a lock-in technique with an excitation voltage amplitude of 70 μV_{RMS} at 928 Hz. Unless specified otherwise, in all measurements the applied magnetic field (up to 9 T) was oriented perpendicular to the sample surface. IETS measurements were performed at intervals of 200 mT, forming a set of 46 spectra per atom (except for the seven-atom chain, for which only 44 spectra up to 8.6 T were performed). To achieve a substantial reduction of the data acquisition time, an automated procedure was developed. After taking spectra on each atom at a given field, the tip returned to the first atom and retracted 2 nm, followed by a 50 mT automated field sweep. Following each sweep, the tip was brought back into the tunnelling range (50 pA, 15 mV), following which potential drift was corrected for through an automated atom-locking procedure. The field should be increased by 50 mT or less in each sweep to avoid the drift being larger than one atom radius. For data such as presented in Figs 2 and 3, IETS measurements were performed after every fourth field sweep to give an interval of 200 mT. Using this method, obtaining a data set for fields ranging from 0 T to 7 T required performing the experiment continuously for 7 h on a single Co atom to 28 h on a $N = 9$ chain. Spectra taken above 7 T were obtained manually for each atom of every chain, owing to tip instabilities disabling proper atom locking when sweeping the field in that range.

Spin-polarized measurements. A spin-filtering tip was created by attaching several Co atoms to the tip and applying a field of 3 T perpendicular to the surface. Spin polarization was verified by performing spectroscopy on a single Co atom. As shown in Supplementary Fig. 4, the relative heights of the peaks were found to be opposite to those recently reported[35], indicating that the ultimate atom of the tip was polarized opposite to the external field owing to exchange forces within the tip.

References

34. Leibsle, F., Flipse, C. & Robinson, A. Structure of the Cu 100 -c(2 × 2)N surface: a scanning-tunneling-microscopy study. *Phys. Rev. B* **47,** 15865–15868 (1993).
35. von Bergmann, K., Ternes, M., Loth, S., Lutz, C. P. & Heinrich, A. J. Spin polarization of the split Kondo state. *Phys. Rev. Lett.* **114,** 076601 (2015).